Quality of Peri-Urban Soil Developed from Ore-Bearing Carbonates: Heavy Metal Levels and Source Apportionment Assessed Using Pollution Indices

Katarzyna Sutkowska [1,*]**, Leslaw Teper** [1]**, Tomasz Czech** [2] **, Tomasz Hulok** [1]**, Michał Olszak** [1] **and Jan Zogala** [1]

[1] Institute of Earth Sciences, University of Silesia in Katowice, Bedzinska 60, 41-200 Sosnowiec, Poland; leslaw.teper@us.edu.pl (L.T.); Thulok@op.pl (T.H.); michal.olszak@outlook.com (M.O.); jan_zogala@o2.pl (J.Z.)

[2] Department of Agricultural and Environmental Chemistry, University of Agriculture in Krakow, Aleja Adama Mickiewicza 21, 31-120 Kraków, Poland; Tomasz.Czech@ur.krakow.pl

* Correspondence: katarzyna.sutkowska@us.edu.pl

Abstract: Pollution indices are used to assess the influence of the bedrock as a natural source of heavy-metal (*HM*), and anthropogenic pollution from ore mining in soils developed from ore-bearing carbonates. The research was conducted in two areas differing in geological setting and type of land use in the Upper Silesia Industrial Region, Southern Poland. Physical properties such as pH, total sulfur, total carbon and total organic carbon values, as well as total Zn, Pb, and Cd contents (ICP-OES) for 39 topsoil samples were measured. Contamination factor (C_f), degree of contamination (C_{deg}), pollution load index (*PLI*) and geoaccumulation index (I_{geo}), were used to determine the deterioration of topsoil due to *HM* pollution. The *HM* content exceeded geochemical background levels by 2.5–18.1 times. Very high to moderate topsoil contamination was determined. In a shallow historical mining zone, the relative influence of particular *HM* was found to be in the order of Pb > Cd > Zn and, in a deep mining zone, Zn > Cd > Pb. In the topsoil developed over shallow ore bodies, the *HM* content was mainly (60%) due to naturally occurring *HM*. In the area of deeply buried ore bodies, 90% of the *HM* load was related to anthropogenic sources. Zn, Pb and Cd vertical distributions and the patterns of topsoil pollution differ in terms of types of mined ores, mining methods and times elapsed since mining ceased. Pollution indices are an efficient tool for distinguishing soil anthropogenic pollution and geogenic contamination.

Keywords: pollution indices; heavy metals; soil contamination; geogenic and anthropogenic origin

1. Introduction

Heavy metals (*HM*) in the environment originate from geological, industrial, agricultural, atmospheric, and waste sources. Soil is one of the most important environmental components at risk of *HM* contamination as a result of anthropogenic activities. A high concentration of *HM*s and metalloids (Zn, Pb, Cd, As, Tl, etc.) can be found in and around active and abandoned mines or smelting plants [1–3] due to the emission and dispersion of pollutants into air [4,5], water [6,7], soil [8–17], plants [4,18–22], and fauna [23,24]. The global average concentration of *HM*s in soils varies for Zn (10–300 mg·kg^{-1}), Pb (10–150 mg·kg^{-1}) and Cd (0.06 mg·kg^{-1}) [25]. In general, the *HM* concentrations in soils are increasing over time, and the highest concentrations are observed in industrial cities, due to traffic, power plants, and other industrial activities [25]. Soil contains baseline or background

concentrations of *HM*. The *HM* content is determined by the composition of the parent rock material from which the soil is derived.

The effective assessment of soil *HM* contamination is an important global issue [10,25–29]. Indicators for the geochemical assessment of the soil environment include contamination factor (C_f), degree of contamination (C_{deg}), pollution load index (*PLI*), and geoaccumulation index (I_{geo}). These indicators enable the estimation of environmental risk and soil degradation due to accumulation of *HM*s [28–30]. Moreover, they facilitate differentiation between the accumulation of *HM*s produced by natural processes and anthropogenic activities (e.g., [31]). Essential to any assessment of the degree of soil contamination is the selection of an appropriate reference value. Although this issue has already been widely discussed [26,32–36], there is still a lack of unambiguous methodological findings.

The aim of the current study is to assess the quality of soil developed from Zn-Pb ore-bearing carbonates, in terms of (1) the influence of the bedrock, as a natural/geogenic source of *HM*s, and (2) anthropogenic pollution from ore mining and processing. We attempted a source apportionment of *HM*s (Zn, Pb, Cd) based on the pollution indices and using the local/on-site geochemical background. The research was carried out on the topsoil layers that are usually expected to accumulate trace elements of anthropogenic origin.

The main novelty of our work consists in taking into account data linking the indices to a broader geological context and mining history which has scarcely been published. We compare two areas located in the same Zn-Pb MVT-type deposit, which differ in terms of types of mined ores, ore-body depth, mining method and the time of mining cessation. The presented approach can be applied to the analyses of environmental risk and *HM* source apportionment in the abandoned mining sites worldwide.

2. Study Area

Two areas located in the north-east part of the Upper Silesia Basin (Figure 2) in the Dlugoszyn and Wilkoszyn Synclines in Jaworzno City were chosen for the study. Both synclines belong to the superior synclinorial structure with an NW-NE trending axis resulting from the Alpine orogenic movements. The inclination of the rock layers varies from 4° to 15° NW in the Dlugoszyn Syncline, and from 4° to 20° SE in the North-West limb of the Wilkoszyn Syncline. These tectonic structures comprise the Middle Triassic carbonate formation, which is composed of dolomites, limestones, and marls. The carbonate rock profile is partially altered due to the epigenetic fluid flow resulting in dolomitisation [37]. The Zn-Pb mineralisation followed the dolomitisation episode, which developed the ore-bearing dolomites with Zn-Pb ore deposits [38]. The Zn-Pb ore deposits in the area belong to the stratabound type. The ore minerals (galena, sphalerite, pyrite, marcasite, and secondary nonsulfides) form bodies of varying horizontal- and vertical extension ranging from several tens of centimetres up to several tens of meters. They consist of metasomatic-, dispersed- and cavity-filling-ores, the latter including crusted-, veined-, drusy- and breccia varieties [39]. Most of the ore bodies have a typical tabular form concordant with the rock bedding. The boundaries between the ore-bearing dolomites and the host carbonate rocks are rarely defined, but more commonly form a broad transition zone into weakly mineralized dolostones.

The areas selected for the study vary in terms of the geological setting. In the Dlugoszyn area (see point 1 in Figures 1 and 2), the ore-bearing dolomites occur near the surface (0–1 m), while in the Wilkoszyn syncline (see point 2 in Figures 1 and 2) the ore bodies occur at a depth of 20 to 90 m. The relatively shallow occurrence of ore mineralisation favours the development of mining. There is evidence of outcrop and underground Zn-Pb ore mining and smelting from the 12th [40] to the 20th century. The shallow ore exploitation in the Dlugoszyn area was completed at the end of the 19th century, while the deep mines and processing plants in the Wilkoszyn area were abandoned in the middle of the 20th century [41,42]. There is evidence of the historical mining and industrial activity in the landscape of the town [43]. Local ore mining left its mark on natural habitats impacting air [44], water [45,46] and soil [2,3,47–49] quality and imposing imprints onto flora [50,51] and fauna [52,53].
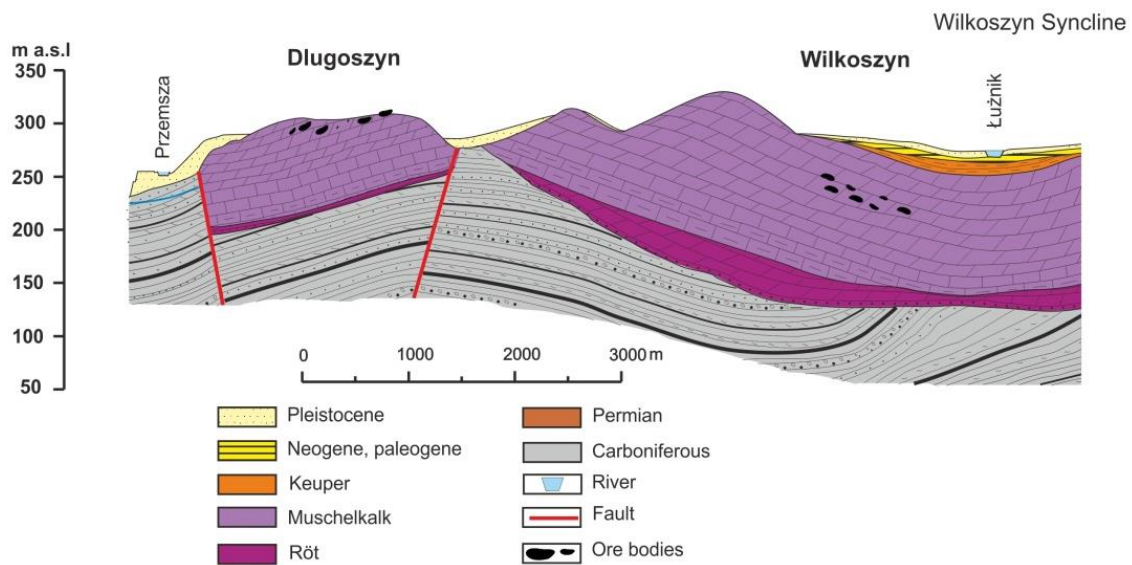
Figure 1. Schematic geological cross-section of the study area showing location of ore bodies, without Quaternary sediments (after [54]).
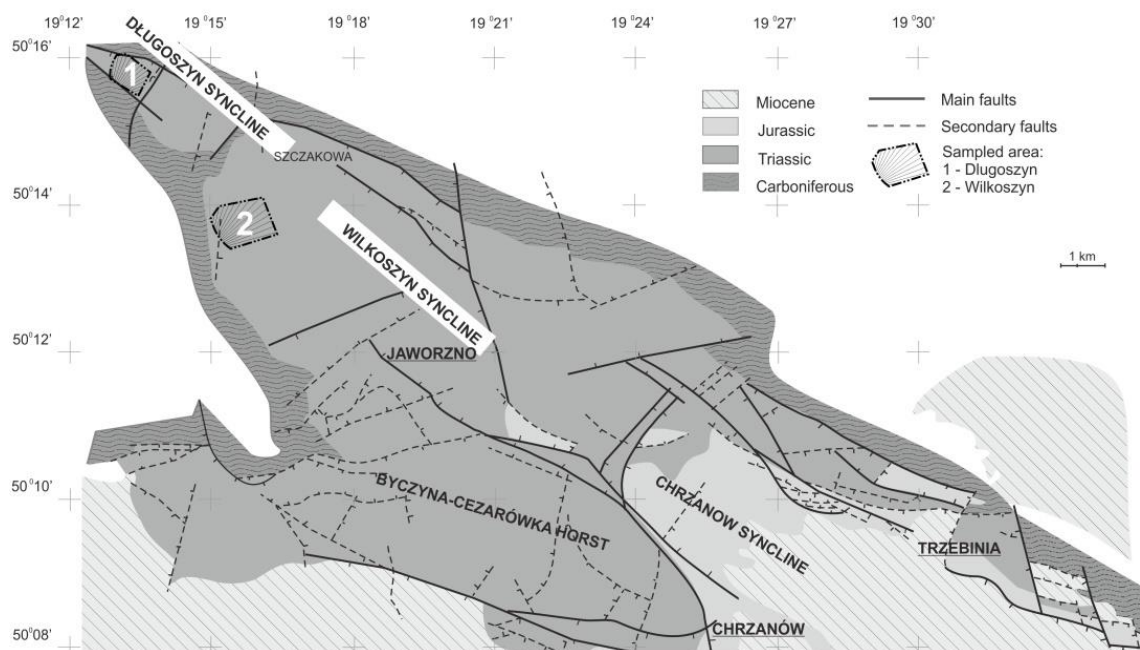

Figure 2. Geological context of the study area, without Quaternary sediments (after [54]).

3. Material and Analytical Methods

To investigate the relationship between the ore-bearing bedrock and content of *HM*s (Zn, Pb, and Cd) in the soils (mostly skeletal Rendzic Leptosol), 15 soil profiles were studied (Figure 3). We tried to select homogenous soil profiles. Each soil profile was divided into separate horizons, providing 54 soil samples. Only the topsoil layers (up to 30 cm depth), characterised by the highest concentrations of *HM*, were considered further; these are represented by 39 soil samples in Table 1. Moreover, bedrock specimens (from each study area) were sampled and analysed to evaluate the local/natural chemical pedogenic enrichment.

Table 1. Geochemical properties of the topsoil samples. D—Dlugoszyn area, W—Wilkoszyn area.

| Sample Point | Coordinates | Sample Number | Depth [cm] | pH | TC [%] | TOC [%] | TS [%] | HM Content [mg·kg⁻¹] | | |
								Zn	Pb	Cd
D1	50°14′19.2″ N 19°14′30″ E	a	0–2	6.40	10.08	9.83	0.11	3329 ± 84	1674 ± 30	37.58 ± 3.27
		b	2–25	7.04	3.29	2.78	0.03	3319 ± 79	1877 ± 39	32.40 ± 1.63
D2	50°14′58.5″ N 19°14′18.7″ E	a	0–2	4.26	20.92	20.92	0.14	701 ± 17	341 ± 6	11.75 ± 0.56
		b	2–9	5.26	9.88	9.88	0.08	907 ± 8	353 ± 3	14.72 ± 0.36
		c	9–19	6.23	1.35	1.35	0.01	482 ± 48	97 ± 10	4.54 ± 0.46
		d	19–26	7.24	0.21	0.20	0.00	277 ± 30	55 ± 8	2.14 ± 0.27
D3	50°15′7.2″ N 19°14′25″ E	a	0–3	6.04	22.01	21.22	0.13	1438 ± 66	234 ± 12	7.46 ± 0.51
		b	3–11	6.65	9.89	7.38	0.04	1291 ± 14	329 ± 0.2	11.29 ± 0.05
		c	11–22	7.03	2.06	1.72	0.01	1170 ± 21	248 ± 0.3	6.99 ± 0.07
D4	50°15′7.1″ N 19°14′33″ E	a	0–2	6.41	8.55	8.50	0.07	1113 ± 12	275 ± 3	9.59 ± 0.45
		b	2–14	6.71	7.14	6.28	0.07	1037 ± 16	269 ± 8	9.50 ± 0.13
		c	14–34	6.91	1.41	1.39	0.01	937 ± 23	227 ± 6	8.11 ± 0.3
D5	50°15′18.2″ N 19°14′25.6″ E	a	0–2	5.55	23.12	23.12	0.17	926 ± 32	283 ± 11	10.46 ± 0.47
		b	2–14	6.06	7.16	7.16	0.07	797 ± 18	267 ± 2	10.45 ± 0.04
		c	14–19	5.96	0.20	0.20	0.00	68 ± 8	18 ± 2	0.31 ± 0.01
W1	50°13′36.1″ N 19°16′48.3″ E	a	0–2	6.74	5.76	5.76	0.06	2975 ± 45	440 ± 2	26.83 ± 0.23
		b	2–18	6.97	3.40	3.40	0.04	3077 ± 54	456 ± 1	27.66 ± 0.13
W2	50°13′36.2″ N 19°16′58.1″ E	a	0–2	6.93	11.57	11.08	0.10	1861 ± 4	673 ± 8	14.45 ± 0.25
		b	2–17	7.36	6.24	5.07	0.05	1831 ± 9	711 ± 6	11.86 ± 0.19
W3	50°13′28.6″ N 19°16′58.7″ E	a	0–2	6.34	9.22	9.22	0.07	2455 ± 34	885 ± 13	17.93 ± 0.14
		b	2–12	6.67	7.47	7.47	0.07	2761 ± 34	1035 ± 18	21.44 ± 0.34
		c	12–24	6.69	0.68	0.68	0.01	1388 ± 2	658 ± 14	3.30 ± 0.01
W4	50°13′27.7″ N 19°16′44.5″ E	a	0–2	6.74	13.89	13.84	0.12	1956 ± 3	329 ± 19	13.70 ± 1.06
		b	2–20	7.08	7.11	7.10	0.07	2547 ± 9	502 ± 6	20.57 ± 0.30
		c	20–30	7.10	2.03	2.03	0.02	2771 ± 27	328 ± 3	12.59 ± 0.31
W5	50°13′27.8″ N 19°16′35.4″ E	a	0–2	7.05	3.49	3.49	0.04	1063 ± 9	403 ± 2	7.42 ± 0.05
		b	2–18	7.24	3.65	3.65	0.04	1052 ± 6	400 ± 14	7.32 ± 0.30
		c	18–28	7.60	0.83	0.82	0.01	1124 ± 48	207 ± 8	4.39 ± 0.21
W6	50°13′9″ N 19°16′11″ E	a	0–3	6.21	2.04	2.04	0.02	630 ± 15	290 ± 4	6.28 ± 0.29
		b	3–11	6.40	1.65	1.65	0.02	583 ± 17	275 ± 5	4.34 ± 0.01
W7	50°13′8″ N 19°15′56″ E	a	0–3	6.99	6.33	6.11	0.07	1063 ± 11	289 ± 1	5.81 ± 0.14
		b	3–19	7.00	3.79	3.70	0.05	1169 ± 1	307 ± 2	7.09 ± 0.02
		c	19–26	7.20	1.45	1.17	0.01	639 ± 1	118 ± 1	2.34 ± 0.01
W8	50°13′15″ N 19°15′56″ E	a	0–4	6.47	3.44	3.44	0.04	1003 ± 3	242 ± 1	4.38 ± 0.03
		b	4–20	6.50	2.78	2.78	0.03	1080 ± 7	298 ± 1	6.05 ± 0.02
W9	50°13′15″ N 19°16′10″ E	a	0–3	6.01	1.59	1.59	0.02	480 ± 9	146 ± 5	3.90 ± 0.04
		b	3–13	6.12	1.60	1.60	0.02	497 ± 2	169 ± 1	3.95 ± 0.01
W10	50°13′25″ N 19°15′59″ E	a	0–3	6.53	2.34	2.34	0.02	652 ± 7	207 ± 2	3.71 ± 0.01
		b	3–17	6.56	2.31	2.31	0.03	727 ± 3	219 ± 1	4.20 ± 0.02

Prior to the analysis, the soil samples were oven-dried at 105 °C to constant weight, sieved to 2 mm through a stainless-steel sieve, and milled into a fine powder, while the bedrock samples were crushed and ground. The soil pH was determined using a 1:5 (g:mL) ratio of soil and 1 M KCl solution, with pH meter ELMETRON CP-315 m. The concentration of total carbon (TC), total organic carbon (TOC), and total sulfur (TS) were determined using an Eltra CS-530 IR-analyser with a TIC module. In order to determine the total content of Zn, Pb, and Cd, the soil and rock samples were wet digested in a closed system in a mixture of 6 cm³ of concentrated nitric acid (65% Suprapur), and 2 cm³ of hydrochloric acid (30% Suprapur). Digestion proceeded with the use of a Perkin Elmer Multiwave 3000 Microwave Digestion, in two steps according to the program of mineralisation recommended by the manufacturer—power: 1400 W, recovery time: 5 min, hold: 25 min in the first step, 10 min in the second, fan speed: 1 in the first step, 3 in the second. After mineralisation, the samples were transferred to measuring flasks (10 cm³) with a 1% solution of Suprapur nitric acid. The *HM* content

in the prepared solution was determined using an atomic emission spectrometer ICP-OES Optima 7300 Dual View Perkin Elmer. Each sample was analysed twice. The quality control procedure was performed using internal laboratory standard for soil material. The percentage recovery for observed elements ranged from 86.5% to 100% (Supplementary Materials Table S1). The ICP-OES analyses were performed at the Department of Agricultural and Environmental Chemistry, University of Agriculture in Krakow.
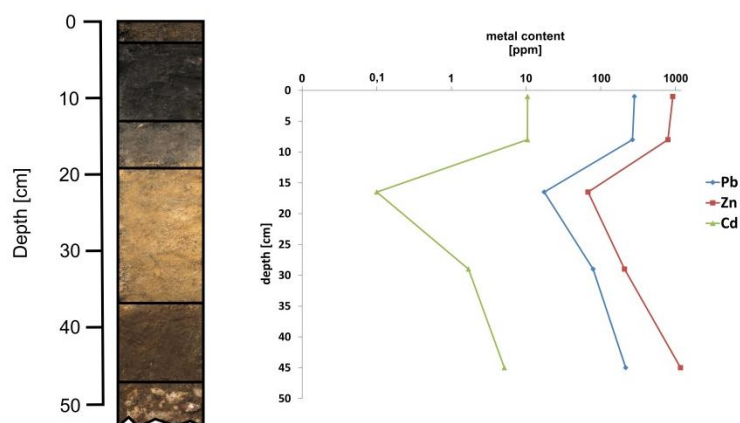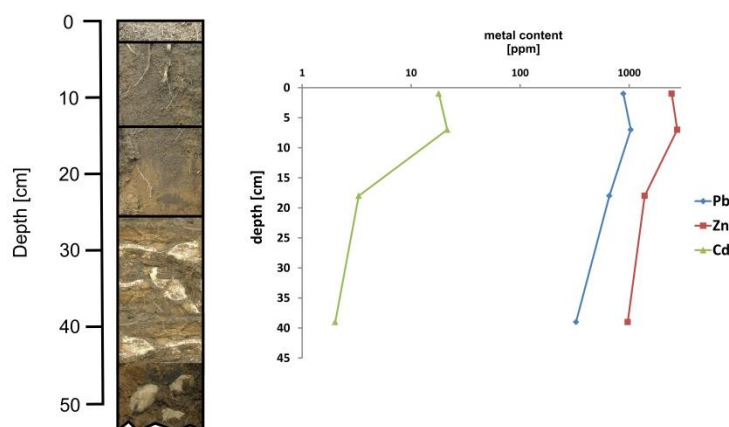

Figure 3. Characteristic examples of studied soil profiles in elevated- (profile D5) and buried (profile W3) ore-bearing dolomitic areas (photographs: T. Hulok).

The phase composition was provided by X-ray diffraction (XRD). The analyses were performed on powdered samples using a PANalytical X'Pert Pro MPD (multipurpose diffractometer) powered by a Philips PW3040/60 X-ray generator and fitted with a 1D silicon strip detector (X'Celerator). The measurements were performed using Co Kα-radiation with a wavelength of 0.1789010 nm, an acceleration voltage of 40 kV, a current of 40 mA, and with 0.02° 2θ step sizes between the angles of 5° and 70° 2θ and a 300 s measurement time per step. The data obtained were processed using HighScore+ software and the ICSD database and PDF4+ ICDD database. All XRD analyses were performed at the Institute of Earth Sciences, Faculty of Natural Sciences, University of Silesia, Sosnowiec.

4. Soil Pollution Assessment

The concentration of *HM*s in the soil is related either to the natural abundance if they come from parent rocks or the anthropogenic load if they come from mining- and processing activities. The distinction between the background of the site level and the pollution load is essential to determine the nature of any anomaly, especially in industrial areas such as the selected study area.

The *HM* contamination in the soil samples is evaluated by applying the C_f, C_{deg}, *PLI*, and I_{geo}.

The C_f is employed to determine the degree of soil pollution with a particular potentially toxic element. The calculation of this factor follows Håkonson's [55] definition (Equation (1)):

$$C_f = \frac{C_{HM}}{C_B},\tag{1}$$

where C_{HM} is the *HM* concentration in soil samples (mg·kg^{-1}) and C_B is reference concentration of *HM*s in soil in the study area (mg·kg^{-1}). According to Håkonson [55], four contamination categories can be distinguished: $C_f < 1$, low; $1 < C_f < 3$, moderate; $3 < C_f < 6$, considerable; and $C_f > 6$, very high contamination.

The estimation of the degree of total contamination of surface layers in a particular core or sampling site was proposed by Håkanson [55] as a sum of the C_f for each sample, or C_{deg} (Equation (2)):

$$C_{deg} = \sum_{i=1}^{i=n} C_f,\tag{2}$$

The classification of the C_{deg} in sediments is as follows [55]: $C_{deg} < 6$, low; $6 < C_{deg} < 12$, moderate; $12 < C_{deg} < 24$, considerable; and $C_{deg} > 24$, high.

The status of the *HM* pollution in the studied soils is assessed through the *PLI* [56]. The *PLI* is calculated by obtaining the *n*-root from the product of *n*- C_f s for all the *HM*s, where n is the number of *HM*s studied (Equation (3)):

$$PLI = \sqrt[n]{(CF_{HM1} \times CF_{HM2} \ldots \times CF_{HMn})},\tag{3}$$

A *PLI* value < 1 indicates minimal or no metal pollution, a *PLI* = 1 indicates that the level of pollutants is equal to the baseline content of *HM*, whereas *PLI* > 1 means that there is pollution and the value indicates the severity of the pollution. For the latter case, Zhang et al. [57] classify soils into the following five categories: $1 < PLI < 2$, moderately; $2 < PLI < 3$, moderately to highly; $3 < PLI < 4$, highly $4 < PLI < 5$, very highly; and *PLI* > 5, extremely polluted.

The I_{geo} proposed by Müller [58] is a common criterion to evaluate the *HM* pollution in sediments/soil. It is defined as follows (Equation (4)):

$$I_{geo} = log_2\left(\frac{C_{HM}}{1.5\,C_B}\right),\tag{4}$$

where C_{HM} is the *HM* concentration in soil samples (mg·kg^{-1}); C_B is reference concentration of *HM*s in the soil in the study area (mg·kg^{-1}), and factor 1.5 is incorporated in the relationship to account for possible variation in background data due to the lithogenic effect. Müller [58] distinguished seven classes of soil quality based on *HM* enrichment: Class 0–$I_{geo} < 0$, uncontaminated; Class 1–$0 < I_{geo} < 1$, uncontaminated to moderately; Class 2–$1 < I_{geo} < 2$, moderately; Class 3–$2 < I_{geo} < 3$, moderately to highly; Class 4–$3 < I_{geo} < 4$, highly; Class 5–$4 < I_{geo} < 5$, highly to extremely; Class 6–$I_{geo} > 5$, extremely contaminated. I_{geo} Class 0 suggests the lack of contamination, while the highest Class 6 shows the extreme enrichment of the *HM*s relative to background values.

The above reference concentration, symbolised as C_B, depends on the local natural conditions, and differs widely from one geologic unit to another. The metal background depends on the

composition of the parent rock from which the soil was derived [13]. Thus, use of Clark values or off-site reference methods are obviously not appropriate, especially in assessing weakly contaminated sites [34]. The on-site reference value is more specific and sensitive in the case of trace-element soil contamination [33]. Because of the bedrock of ore-bearing dolomites in the research area, we decided to use the *HM* content in the carbonate bedrock (Table 2) as a local reference value. In addition, three more off-site reference values (Table 2) were applied to further define the role played by different sources in the topsoil contamination detected.

Table 2. HM concentrations in topsoil samples and baseline CB values (mg·kg^{-1} dry weight).

Sample Point	Weighted Arithmetic Mean (mg·kg^{-1} Dry Weight)			Statistical Parameters				
	Zn	**Pb**	**Cd**			**Zn**	**Pb**	**Cd**
D1	3320	1861	32.82	content	min.	68	18	0.31
D2	558	173	7.19		max.	3329	1877	37.58
D3	1251	275	8.62	weighted arithmetic mean		1351	550	13.01
D4	982	244	8.69	median		937	269	9.59
D5	619	203	7.73	standard deviation		910	535	9.83
				coefficient of variation [%]		77	123	83.29
W1	3066	454	27.57					
W2	1159	492	7.04					
W3	1032	361	4.14					
W4	2582	432	17.45			**Zn**	**Pb**	**Cd**
W5	1054	340	7.34	content	min.	480	118	2.34
W6	595	279	4.87		max.	3077	1035	27.66
W7	1014	254	5.66	weighted arithmetic mean		1549	410	10.43
W8	1149	331	4.43	median		1102	317	6.68
W9	287	87	2.29	standard deviation		849	232	7.53
W10	714	217	4.11	coefficient of variation [%]		1102	317	6.68
baseline C_B values								
	Zn	**Pb**	**Cd**					
1	552	61	3.41	carbonate bedrock for Dlugoszyn area				
2	86	81	1.22	carbonate bedrock for Wilkoszyn area				
3	104	44	1.30	median for topsoil for S Poland [59]				
4	200	84	2	median for topsoil in Cracow-Silesia region [60]				
5	48	15	0.15	median for topsoil in Europe [61]				

5. Results and Discussion

The pH values of the soil in the Dlugoszyn area (Table 1) fluctuate between 4.26 and 7.24 (median 6.57), while in the Wilkoszyn area, the pH varies from 6.01 to 7.6 (median 6.77), indicating that the examined soil samples are extremely acidic to slightly alkaline, but mostly neutral. Generally, the pH value decreases with depth. The TOC values obtained for the soil range from 0.2% to 23.12% (median 1.72%) in the Dlugoszyn area and from 0.68% to 13.84% (median 2.04%) in the second study area, while TS varies from 0 to 0.14% (median 0.01%) and 0.01 to 0.12% (median 0.02%), in the two study areas, respectively (Table 1). Both parameters diminish with depth. The TOC levels observed are characteristic for rendzina skeletal soils.

The concentrations of Zn, Pb, and Cd in the soil differ significantly between the elevated (Dlugoszyn) and buried (Wilkoszyn) ore-bearing dolomite areas (Table 2). The Dlugoszyn soil samples contain 68–3329 mg·kg^{-1} d.m. of Zn, 18–1877 mg·kg^{-1} d.m. of Pb, and 0.31–37.58 mg·kg^{-1} d.m. of Cd, with weighted arithmetic means 1351 mg·kg^{-1} d.m., 550 mg kg^{-1} d.m., and 13.01 mg·kg^{-1} d.m., respectively. The pollution load of the same elements in the Wilkoszyn area ranges as follows: 480–3077 mg·kg^{-1} d.m. for Zn, 118–1035 mg·kg^{-1} d.m. for Pb, and 2.34–27.66 mg·kg^{-1} d.m. for Cd, with weighted arithmetic means 1549 mg·kg^{-1} d.m., 410 mg·kg^{-1} d.m., and 10.43 mg·kg^{-1} d.m., respectively. For the soil derived from ore-bearing dolomites occurring close to the surface in the Dlugoszyn area, the mean concentrations of the studied metals exceed 2.5-, 9- and 3.8-fold of the Zn, Pb, and Cd content in bedrock, respectively. For the soil developed in the Wilkoszyn area from deeper ore-bearing dolomites, the mean values calculated are 18.1- (for Zn), 5.1- (for Pb), and 8.6-fold (for Cd) higher than the baseline level (compare Table 2), indicating intensive soil contamination in both study areas.

The main crystalline phases in the topsoil are in the 79.5–84 wt.% (Table 3) represented by quartz (Figure 4). Goethite is abundant, especially in the Wilkoszyn area (11.5 wt.%). The large concentration of dolomite (3–5%), and some calcite (to 0.5 wt.%) were also detected. The K-feldspars (microcline and orthoclase), albite, plagioclases, and kaolinite occur there as the accessory minerals. The low-crystalline goethite (7.16Å in Figure 4), is accompanied by amorphous iron oxides or sulfides (marcasite, hematite—2.695 Å) and/or iron oxide/hydroxide. Additionally, the pyroxene (augite-diopside) or spinel Zn-Al-Fe family phases were documented by diffraction peak 4.675 Å.

Table 3. Semiquantitative mineralogical analysis of XRD results.

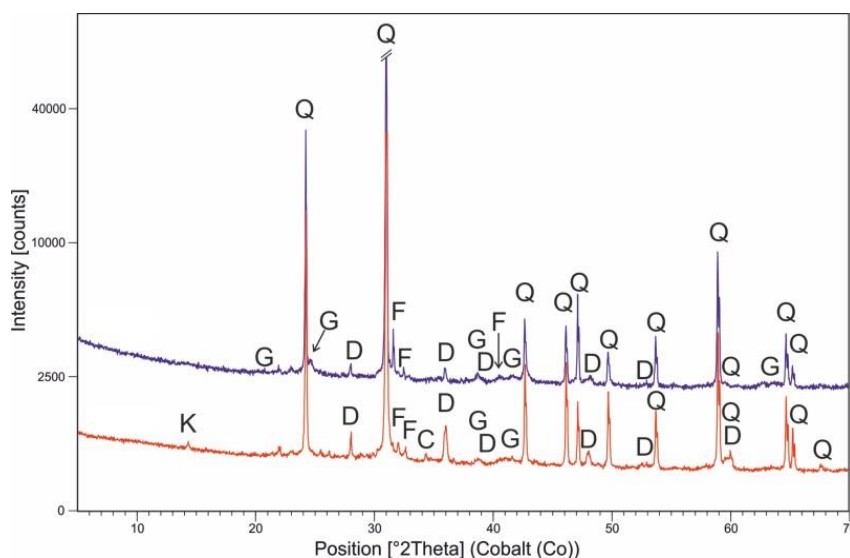| Mineral Name	D Area	W Area
	[%]	
Quartz	84.0	79.5
Dolomite	4.5	3.0
Goethite	0.5	11.5
Microcline	3.0	2.5
Orthoclase	3.0	1.0
Albite	2.5	2.5
Kaolinite	2.0	-
Calcite	0.5	-

Figure 4. XRD patterns of topsoil from D-Dlugoszyn (red line) and W-Wilkoszyn (blue line) area. Symbol explanations: C—calcite, D—dolomite, F—feldspars, G—goethite, Q—quartz.

On the basis of the trace-element contents of the sampled soil, the natural concentration and the contamination from anthropogenic sources cannot be distinguished. To assess the degree of anthropogenic influence on the soils, the selected pollution indices (C_f, C_{deg}, *PLI*, and I_{geo}) were calculated.

The C_f was calculated for each soil sample relative to the bedrock value for both study areas (Table 2). The C_f of Zn, Pb, and Cd in the Dlugoszyn area is in the range of 1.0–6.0, 2.8–30.6, and 2.1–9.6, with a mean value of 2.4, 9.1, and 3.8, respectively (Table 4). This indicates considerable to very high (80% of results for Pb) and moderate to considerable (100% for Zn and 80% for Cd) topsoil contamination level (Table 5). In the Wilkoszyn area, C_f has values of 6.9–35.8, 1.1–6.1 and 1.9–22.6 for Zn, Pb, and Cd, respectively, with a mean value of 14.8, 4.1, and 7.0, respectively (Table 4). Such C_f levels point to considerable to very high contamination degree with Zn (100% of results) and Cd (90%), and moderate to considerable pollution with Pb (80%) (Table 5).

Table 4. Assessment of *HM* pollution indices in studied topsoil in relation to the local carbonate bedrock in the D-Dlugoszyn and W-Wilkoszyn areas as a background value.

Sample Point	C_f			C_{deg}	PLI	I_{geo}		
	Zn	**Pb**	**Cd**			**Zn**	**Pb**	**Cd**
D1	**6.0**	**30.6**	**9.6**	**46.2**	**12.1**	2.0	**4.3**	2.7
D2	1.0	2.8	2.1	6.0	1.8	−0.6	0.9	0.5
D3	2.3	**4.5**	2.5	9.3	3.0	0.6	1.6	0.8
D4	1.8	**4.0**	2.5	8.3	2.6	0.2	1.4	0.8
D5	1.1	**3.3**	2.3	6.7	2.0	−0.4	1.2	0.6
W1	**35.8**	**5.6**	**22.6**	**64.0**	**16.5**	**4.6**	1.9	**3.9**
W2	**13.5**	**6.1**	**5.8**	**25.4**	**7.8**	**3.2**	2.0	1.9
W3	**12.0**	**4.5**	**3.4**	**19.9**	**5.7**	**3.0**	1.6	1.2
W4	**30.1**	**5.3**	**14.3**	**49.8**	**13.2**	**4.3**	1.8	**3.3**
W5	**12.3**	**4.9**	**6.0**	**23.2**	**7.1**	**3.0**	1.7	2.0
W6	**6.9**	**3.4**	**4.0**	**14.4**	**4.6**	**2.2**	1.2	1.4
W7	**11.8**	**3.1**	**4.6**	**19.6**	**5.6**	**3.0**	1.1	1.6
W8	**13.4**	**4.1**	**3.6**	**21.1**	**5.8**	**3.2**	1.4	1.3
W9	**3.3**	1.1	1.9	6.3	1.9	1.2	−0.5	0.3
W10	**8.3**	2.7	**3.4**	**14.4**	**4.2**	**2.5**	0.8	1.2

In bold—strongly contaminated.

The C_{deg} index determines the degree of overall contamination of a particular sample in the study areas. Based on the C_{deg} (see Tables 4 and 5), 80% of the calculated values for the Dlugoszyn samples are recognised as moderately contaminated, while 20% are very highly contaminated. In the Wilkoszyn samples, 60% indicate very high (30%) and moderate (10%) pollution of the topsoil (Table 5).

The PLI indicates deterioration of the soil quality due to metal pollution. In the current study, the PLI obtained for the Dlugoszyn samples indicates moderate (20% of results), moderate to high (40%), high (20%) and extreme (20%) topsoil pollution (Table 5), with values ranging from 1.8 to 12.1, and mean equal to 4.3 (Table 4). In the Wilkoszyn samples, the PLI values range from 1.9 to 16.5, with a mean of 7.2 (Table 4) pointing to extremely (70% of results), very high (20%), and moderately (10%) polluted topsoil (Table 5).

The pollution indices indicate the moderately to extremely high level of topsoil contamination and reveal a difference in the level of topsoil contamination between the study areas (Table 5).

Table 5. Percentage of class distribution of topsoil pollution for indices considered. D—Dlugoszyn area, W—Wilkoszyn area.

Pollution Index	Classes of Soil Quality	Studied Area					
		D			W		
		Zn	Pb	Cd	Zn	Pb	Cd
C_f [%]	very high contamination	0	20	20	90	10	20
	considerable contamination	20	60	0	10	70	70
	moderate contamination	80	20	80	0	20	10
	low contamination	0	0	0	0	0	0
C_{deg} [%]	very high contamination	20			30		
	considerable contamination	0			60		
	moderate contamination	80			10		
	low contamination	0			0		
PLI [%]	extremely high pollution	20			70		
	very high pollution	0			20		
	high pollution	20			0		
	moderate to high pollution	40			0		
	moderate pollution	20			10		
	unpolluted	0			0		
I_{geo} [%]	Class 6 extremely polluted	0	0	0	0	0	0
	Class 5 highly to extremely polluted	0	20	0	20	0	0
	Class 4 heavy polluted	0	0	0	50	0	0
	Class 3 moderately to heavily polluted	20	0	20	20	10	30
	Class 2 moderately polluted	0	60	0	10	70	60
	Class 1 unpolluted to moderately polluted	40	20	80	0	10	10
	Class 0 unpolluted	40	0	0	0	10	0

The I_{geo} ranges from −0.6 to 2.0 for Zn, with a mean value of 0.4; 0.9 to 4.3 for Pb, with a mean value of 1.9, and 0.5 to 2.7 for Cd, with a mean value of 1.1 in the Dlugoszyn area (Table 4). The values of I_{geo} for *HM*s decrease in the sequence Pb > Cd > Zn. The results classify the area as highly polluted with Pb and moderately polluted with Zn and Cd (Table 5). In contrast, in the Wilkoszyn area, the I_{geo} varies widely from 1.2–4.6 for Zn, with mean value 3.0; −0.5–2.0 for Pb, with mean value 1.3 and 0.3–3.9 for Cd, with mean value 1.8 (Table 4). The *HM* pollution follows the order Zn > Cd > Pb. Using I_{geo}, we can determine the potential source of pollution. The I_{geo} values obtained for the elevated ore-bearing dolomites in the Dlugoszyn area indicate mainly baseline levels of pollution for Zn and Cd, as 80% Zn and 80% Cd belong to Classes 0 and 1. The only exception is pollution with Pb (see Table 5). Most of the Zn and Cd are derived from geogenic sources, and most of the Pb (80%) is derived from anthropogenic sources. As such, in the Dlugoszyn area, the deterioration in soil quality is due to Pb. In the Wilkoszyn area, with buried ore-bearing dolomites, moderate to heavy pollution by Pb and Cd is observed, as 80% Pb and 90% Cd belong to Class 2 and 3 (Table 5). Heavy to extreme pollution by Zn is identified, as 70% Zn belongs to Class 4 and 5 (Table 5). Based on these results and the fact that concentrations of *HM*s decrease with depth, the *HM*s in the topsoil of the Wilkoszyn location is of anthropogenic origin. The graphical model of *HM* immissions into the topsoil of the Dlugoszyn and Wilkoszyn areas is presented in the Figure 5, while the complete set of soil profiles studied is put into the Supplementary Materials (Figure S1).

When calculating pollution indices, the selection of an appropriate reference value is an important and complicated issue. Opinions about the best value to use are divided. Some researchers favour the trace-element contents in the deeper soil horizon [32,36,62] or the average values in soil from the study area [30,63] as correct. Others consider the trace-element contents in the bedrock [64,65] as best. The accuracy and sensitivity of the on-site reference value in identifying trace-element soil contamination was evaluated by Desaules [33]. The specific geological setting of both study areas forced us to calculate the selected pollution indices with reference to the bedrock.
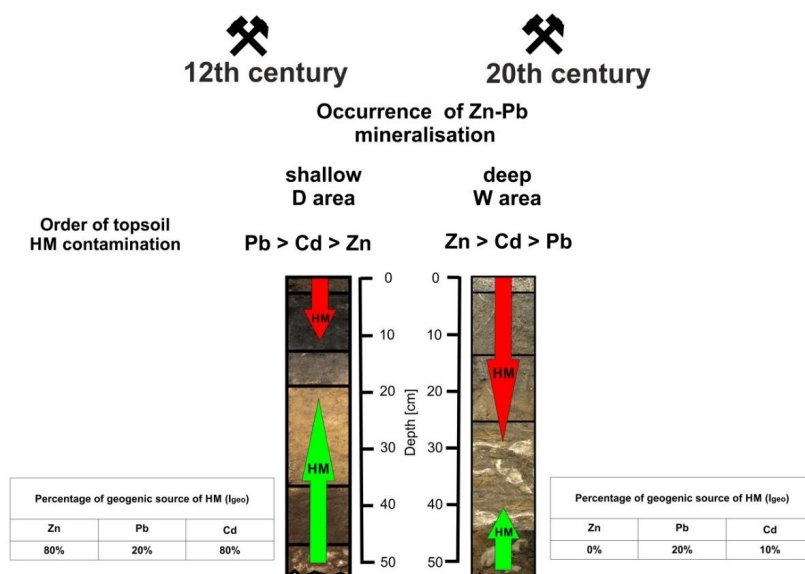
Figure 5. Graphical model of anthropogenic (red arrows) and geogenic (green arrows) *HM* immissions into the topsoil of the D-Dlugoszyn and W-Wilkoszyn areas.

We also take off-site reference values defined as the median for topsoil in (1) the Cracow-Silesia region [60], (2) S Poland [59] and (3) Europe [61] into consideration. Outcomes of these examination are listed in Tables 6–8. In applying the off-site reference values to topsoil in the area where shallow ore-bearing dolomites occur (the Dlugoszyn area), a significantly higher degree of contamination is observed. Additionally, anthropogenic sources are mainly responsible for the *HM* presence in the soil. The percentage of class distribution shows (Tables 6–8) that 80–100% of I_{geo} values belong to classes 2–6. The only exception refers to Pb when the S Poland median value is used. In the case of deeper situated Zn-Pb mineralization (the Wilkoszyn area), comparable results were obtained using the off-site and on-site reference values. Significant differences were noted when the reference value for European topsoil was considered. Using the latter reference value, the extremely high soil contamination (C_f, C_{deg}) here is attributed mainly to human activity (I_{geo}; see Table 8). In our opinion, and especially in the case where the ore-bearing dolomite is near surface, use of the local reference value to assess topsoil contamination provides more reliable results than use of off-site reference values.

Table 6. Assessment of *HM* pollution indices in studied topsoil in relation to the median for topsoil in the Cracow-Silesia region as a background value [60].

Sample Point	C_f			C_{deg}	PLI	I_{geo}		
	Zn	Pb	Cd			Zn	Pb	Cd
D1	**31.9**	**42.3**	**25.2**	**99.5**	**32.4**	**4.4**	**4.8**	**4.1**
D2	**5.4**	**3.9**	**5.5**	**14.8**	**4.9**	**1.8**	**1.4**	**1.9**
D3	**12.0**	**6.3**	**6.6**	**24.9**	**7.9**	**3.0**	**2.1**	**2.1**
D4	**9.4**	**5.6**	**6.7**	**21.7**	**7.1**	**2.7**	**1.9**	**2.2**
D5	**5.9**	**4.6**	**5.9**	**16.5**	**5.5**	**2.0**	**1.6**	**2.0**
W1	**29.5**	**10.3**	**21.2**	**61.0**	**18.6**	**4.3**	**2.8**	**3.8**
W2	**11.1**	**11.2**	**5.4**	**27.7**	**8.8**	**2.9**	**2.9**	**1.9**
W3	**9.9**	**8.2**	**3.2**	**21.3**	**6.4**	**2.7**	**2.5**	**1.1**
W4	**24.8**	**9.8**	**13.4**	**48.1**	**14.8**	**4.0**	**2.7**	**3.2**
W5	**10.1**	**9.1**	**5.6**	**24.9**	**8.0**	**2.8**	**2.6**	**1.9**
W6	**5.7**	**6.3**	**3.7**	**15.8**	**5.1**	**1.9**	**2.1**	**1.3**
W7	**9.7**	**5.8**	**4.4**	**19.9**	**6.3**	**2.7**	**1.9**	**1.5**
W8	**11.0**	**7.5**	**3.4**	**22.0**	**6.6**	**2.9**	**2.3**	**1.2**
W9	2.8	2.0	1.8	6.5	**2.1**	0.9	0.4	0.2
W10	**6.9**	**4.9**	**3.2**	**15.0**	**4.7**	**2.2**	**1.7**	**1.1**

In bold—strongly contaminated.

Table 7. Assessment of *HM* pollution indices in studied topsoil in relation to the median for topsoil in S Poland as a background value [59].

Sample Point	C_f			C_{deg}	PLI	I_{geo}		
	Zn	**Pb**	**Cd**			**Zn**	**Pb**	**Cd**
D1	**16.6**	**22.1**	**16.4**	55.2	18.2	3.5	3.9	3.5
D2	2.8	2.1	**3.6**	8.4	2.7	0.9	0.5	1.3
D3	**6.3**	**3.3**	**4.3**	13.8	4.5	2.1	1.1	1.5
D4	**4.9**	2.9	**4.3**	12.2	4.0	1.7	1.0	1.5
D5	**3.1**	2.4	**3.9**	9.4	3.1	1.0	0.7	1.4
W1	**5.4**	**13.8**	**15.3**	34.5	10.5	3.4	1.9	3.2
W2	**5.9**	**3.5**	**5.8**	15.2	4.9	2.0	2.0	1.2
W3	**4.3**	2.1	**5.2**	11.5	3.6	1.8	1.5	0.5
W4	**5.1**	**8.7**	**12.9**	26.8	8.3	3.1	1.8	2.5
W5	**4.8**	**3.7**	**5.3**	13.7	4.5	1.8	1.7	1.3
W6	3.0	**3.3**	2.4	8.7	2.9	1.0	1.1	0.7
W7	**5.1**	3.0	2.8	10.9	3.5	1.8	1.0	0.9
W8	**5.7**	**3.9**	2.2	11.9	3.7	1.9	1.4	0.6
W9	1.4	1.0	1.1	3.6	1.2	−0.1	−0.5	−0.4
W10	**3.6**	2.6	2.1	8.2	2.7	1.3	0.8	0.5

In bold—strongly contaminated.

Table 8. Assessment of *HM* pollution indices in studied topsoil in relation to the median for European topsoil as a background value [61].

Sample Point	C_f			C_{deg}	PLI	I_{geo}		
	Zn	**Pb**	**Cd**			**Zn**	**Pb**	**Cd**
D1	**69.2**	**124.0**	**218.8**	412.0	123.4	5.5	6.4	7.2
D2	**11.6**	**11.5**	**47.9**	71.1	18.6	3.0	2.9	5.0
D3	**26.1**	**18.4**	**57.4**	101.9	30.2	4.1	3.6	5.3
D4	**20.5**	**16.3**	**57.9**	94.7	26.8	3.8	3.4	5.3
D5	**12.9**	**13.5**	**51.5**	78.0	20.8	3.1	3.2	5.1
W1	**63.9**	**30.3**	**183.8**	278.0	70.9	5.4	4.3	6.9
W2	**24.2**	**32.8**	**46.9**	103.9	33.4	4.0	4.5	5.0
W3	**21.5**	**24.1**	**27.6**	73.2	24.3	3.8	4.0	4.2
W4	**53.8**	**28.8**	**116.4**	199.0	56.5	5.2	4.3	6.3
W5	**21.9**	**26.7**	**48.9**	97.5	30.6	3.9	4.2	5.0
W6	**12.4**	**18.6**	**32.5**	63.5	19.6	3.0	3.6	4.4
W7	**21.1**	**16.9**	**37.8**	75.8	23.8	3.8	3.5	4.7
W8	**23.9**	**22.0**	**29.6**	75.5	25.0	4.0	3.9	4.3
W9	**6.0**	**5.8**	**15.3**	27.0	8.1	2.0	1.9	3.3
W10	**14.9**	**14.5**	**27.4**	56.7	18.1	3.3	3.3	4.2

In bold—strongly contaminated.

Diatta et al. [9] observed similar results, with significantly high *HM* levels in soils impacted by the Miasteczko Slaskie Zn smelter, in part of the Upper Silesia Industrial Region. The mean Zn, Pb, and Cd contents in mg·kg^{-1} reported are 1062.97, 781.91, and 12.32, respectively. Using the off-site reference value to I_{geo}, C_f, and C_{deg} calculations, extremely high contamination was observed for Zn, Cd, and Pb, in ascending order [9]. Our findings differ slightly in terms of the influence of particular *HM*s. In our opinion, the difference between the orders of pollutant intensity acquired for individual sites resulted primarily from the local industrial land use and the kind of reference value.

The historical mining of Zn-Pb ores in the Dlugoszyn area was based on the dominant mineral, galena (Pb sulfide), which occurs in shallow ore bodies which are easily recognised. Moreover, Pb has a relatively low melting point, allowing for ease of processing [41]. As such, ore mining in the area started in the early medieval period and resulted in the most severe Pb pollution in the Dlugoszyn topsoil. The levels of Zn and Cd are derived from the metal-rich bedrock.

The very high Zn and Pb contamination observed in the Wilkoszyn area probably results from the 20th century underground Zn-Pb ore mining and processing, when galena, Zn sulfides, and nonsulfides were mined and processed in the area. As such, it seems probable that recent industrial operations are a principal cause of the high levels of Zn and Pb accumulated in the Wilkoszyn topsoil.

Generally, soil samples from arable fields and home gardens across the Upper Silesia Industrial Region are characterised by high levels of toxic *HM*s. This is reflected in the *HM* concentrations in locally cultivated vegetables, which are well above the permissible levels [11]. Both study areas are used as peri-urban agricultural lands. The very high topsoil *HM* levels reported in this paper are not as harmful due to the pH value (Table 1) observed in studied soil. The *HM*s are regarded as highly soluble and more toxic in an acidic soil environment [66,67].

6. Conclusions

The application of various pollution indices (C_f, C_{deg}, *PLI*, and I_{geo}) and the local background value C_B enable the detection of Zn, Pb, and Cd pollution in soils. Depending on the index used, we determined very high to considerable (according to the classification proposed by [55]) topsoil contamination. The influence intensity of particular metals differs between studied areas. In the case of shallow historical mining (the Dlugoszyn area), it follows the order Pb > Cd > Zn, while in the place of deep mining and processing (the Wilkoszyn area) it decreases in the sequence Zn > Cd > Pb. With the geo-accumulation index, it is possible to discriminate between natural and anthropogenic *HM*s in the soils developed over the ore-bearing formation in the two areas. Based on I_{geo} values, we consider that the *HM* content in the topsoil developed over the shallowly occurring ore bodies in dolomites (the Dlugoszyn area) is mainly (60%) connected with the natural presence of metals. In the Wilkoszyn area where ore bodies are more deeply buried, 90% of the *HM* load is related to anthropogenic sources. An accurate assessment of soil quality, based on *HM* content, is possible only with the combined use of various pollution indices.

References

1. Norgate, T.E.; Jahanshahi, S.; Rankin, W.J. Assessing the environmental impact of metal production processes of metal production processes. *J. Clean. Prod.* **2007**, *15*, 838–848. [CrossRef]

2. Chrastný, V.; Vaněk, A.; Teper, L.; Cabala, J.; Procházka, J.; Pechar, L.; Drahota, P.; Penížek, V.; Komárek, M.; Novák, M. Geochemical position of Pb, Zn and Cd in soils near the Olkusz mine/smelter, South Poland: Effects of land use, type of contamination and distance from pollution source. *Environ. Monit. Assess.* **2012**, *184*, 2517–2536. [CrossRef]

3. Vaněk, A.; Chrastný, V.; Komárek, M.; Penížek, V.; Teper, L.; Cabala, J.; Drábek, O. Geochemical position of thallium in soils from a smelter-impacted area. *J. Geochem. Explor.* **2013**, *124*, 176–182. [CrossRef]

4. Kalinovic, T.S.; Serbula, S.M.; Radojevic, A.A.; Kalinovic, J.V.; Steharnik, M.M.; Petrovic, J.V. Elder, linden and pine biomonitoring ability of pollution emitted from the copper smelter and the tailings ponds. *Geoderma* **2016**, *262*, 266–275. [CrossRef]

5. Ghayoraneh, M.; Qishlaqi, A. Concentration, distribution and speciation of toxic metals in soils along a transect around a Zn/Pb smelter in the northwest of Iran. *J. Geochem. Explor.* **2017**, *180*, 1–14. [CrossRef]

6. Varol, M. Assessment of heavy metal contamination in sediments of the Tigris River (Turkey) using pollution indices and multivariate statistical techniques. *J. Hazard. Mater.* **2011**, *195*, 355–364. [CrossRef] [PubMed]

7. Ogbeibu, A.E.; Omoigberale, M.O.; Ezenwa, I.M.; Eziza, J.O.; Igwe, J.O. Using pollution load index and geoaccumulation index for the assessment of heavy metal pollution and sediment quality of the Benin River, Nigeria. *Nat. Environ.* **2014**, *2*, 1–9. [CrossRef]

8. Loska, K.; Wiechuła, D.; Korus, I. Metal contamination of farming soils affected by industry. *Environ. Int.* **2004**, *30*, 159–165. [CrossRef]

9. Diatta, J.B.; Chudzinska, E.; Wirth, S. Assessment of heavy metal contamination of soils impacted by a zinc smelter activity. *J. Elementol.* **2008**, *13*, 5–16.

10. Li, Z.; Ma, Z.; van der Kuijp, T.J.; Yuan, Z.; Huang, L. A review of soil heavy metal pollution from mines in China: Pollution and health risk assessment. *Sci. Total Environ.* **2014**, *468–469*, 843–853. [CrossRef]

11. Dziubanek, G.; Piekut, A.; Rusin, M.; Baranowska, R.; Hajok, I. Contamination of food crops grown on soils with elevated heavy metals content. *Ecotoxicol. Environ. Saf.* **2015**, *118*, 183–189. [CrossRef] [PubMed]

12. Ettler, V. Soil contamination near non-ferrous metal smelters: A review. *Appl. Geochem.* **2016**, *64*, 56–74. [CrossRef]

13. Nouri, M.; Haddioui, A. Assessment of metals contamination and ecological risk in ait Ammar abandoned iron mine soil, Morocco. *Ekológia* **2016**, *35*, 32–49. [CrossRef]

14. Obiora, S.C.; Chukwu, A.; Davies, T.C. Heavy metals and health risk assessment of arable soils and food crops around Pb-Zn mining localities in Enyigba, southeastern Nigeria. *J. Afr. Earth Sci.* **2016**, *116*, 182–189. [CrossRef]

15. Xue, S.; Shi, L.; Wu, C.; Wu, H.; Qin, Y.; Pan, W.; Hartley, W.; Cui, M. Cadmium, lead, and arsenic contamination in paddy soils of a mining area and their exposure effects on human HEPG2 and keratinocyte cell-lines. *Environ. Res.* **2017**, *156*, 23–30. [CrossRef] [PubMed]

16. Liu, J.; Wang, J.; Xiao, T.; Bao, Z.; Lippold, H.; Luo, X.; Yin, M.; Ren, J.; Chen, Y.; Linghu, W. Geochemical dispersal of thallium and accompanying metals in sediment profiles from a smelter-impacted area in South China. *Appl. Geochem.* **2018**, *88*, 239–246. [CrossRef]

17. Wu, J.; Long, J.; Liu, L.; Li, J.; Liao, H.; Zhang, M.; Zhao, C.; Wu, Q. Risk assessment and source identification of toxic metals in the agricultural soil around a Pb/Zn mining and smelting area in Southwest China. *Int. J. Environ. Res. Public Health* **2018**, *15*, 1838. [CrossRef]

18. Wiggenhauser, M.; Bigalke, M.; Imseng, M.; Müller, M.; Keller, A.; Murphy, K.; Kreissig, K.; Rehkämper, M.; Wilcke, W.; Frossard, E. Cadmium isotope fractionation in soil-wheat systems. *Environ. Sci. Technol.* **2016**, *50*, 9223–9231. [CrossRef]

19. Dinis, L.; Savard, M.M.; Gammon, P.; Bégin, C.; Vaive, J. Influence of climatic conditions and industrial emissions on spruce tree-ring Pb isotopes analyzed at ppb concentrations in the Athabasca oil sands region. *Dendrochronologia* **2016**, *37*, 96–106. [CrossRef]

20. Wei, X.; Lyu, S.; Yu, Y.; Wang, Z.; Liu, H.; Pan, D.; Chen, J. Phylloremediation of air pollutants: Exploiting the potential of plant leaves and leaf-associated microbes. *Front. Plant Sci.* **2017**, *28*, 1318. [CrossRef]

21. Liu, J.; Wei, X.; Zhou, Y.; Tsang, D.C.W.; Bao, Z.; Yin, M.; Lippold, H.; Yuan, W.; Wang, J.; Feng, Y.; et al. Thallium contamination, health risk assessment and source apportionment in common vegetables. *Sci. Total Environ.* **2020**, *703*, 135547. [CrossRef] [PubMed]

22. Wang, J.; Jiang, Y.; Sun, J.; She, J.; Yin, M.; Fang, F.; Xiao, T.; Song, G.; Liu, J. Geochemical transfer of cadmium in river sediments near a lead-zinc smelter. *Ecotoxicol. Environ. Saf.* **2020**, *196*, 110529. [CrossRef] [PubMed]

23. Durkalec, M.; Szkoda, J.; Kolacz, R.; Opalinski, S.; Nawrocka, A.; Zmudzki, J. Bioaccumulation of Lead, Cadmium and Mercury in Roe Deer and Wild Boars from areas with different levels of toxic metal pollution. *Int. J. Environ. Res.* **2015**, *9*, 205–212. [CrossRef]

24. Kapusta, P.; Sobczyk, Ł. Effects of heavy metal pollution from mining and smelting on enchytraeid communities under different land management and soil conditions. *Sci. Total Environ.* **2015**, *536*, 517–526. [CrossRef]

25. Weissmannová, H.D.; Pavlovský, J. Indices of soil contamination by heavy metals—Methodology of calculation for pollution assessment (minireview). *Environ. Monit. Assess.* **2017**, *189*, 616. [CrossRef]

26. Barbieri, M. The importance of enrichment factor (EF) and geoaccumulation index (I_{geo}) to evaluate the soil contamination. *J. Geol. Geophys.* **2016**, *5*, 237. [CrossRef]

27. Baran, A.; Wieczorek, J. Application of geochemical and ecotoxicity indices for assessment of heavy metals content in soils. *Arch. Environ. Prot.* **2015**, *41*, 54–63. [CrossRef]

28. Baran, A.; Wieczorek, J.; Mazurek, R.; Urbański, K.; Klimkowicz-Pawlas, A. Potential ecological risk assessment and predicting zinc accumulation in soils. *Environ. Geochem. Health* **2018**, *40*, 435–450. [CrossRef]

29. Wieczorek, J.; Baran, A.; Urbański, K.; Mazurek, R.; Klimowicz-Pawlas, A. Assessment of the pollution and ecological risk of lead and cadmium in soils. *Environ. Geochem. Health* **2018**, *40*, 2325–2342. [CrossRef]

30. Zang, Z.; Li, Y.; Li, H.; Guo, Z.; Zhang, R. Spatiotemporal variation and pollution assessment of Pb/Zn from smelting activities in China. *Int. J. Environ. Res. Public Health* **2020**, *17*, 1968. [CrossRef]

31. Mazurek, R.; Kowalska, J.B.; Gąsiorek, M.; Zadrożny, P.; Wieczorek, J. Pollution indices as comprehensive tools for evaluation of the accumulation and provenance of potentially toxic elements in soils in Ojców National Park. *J. Geochem. Explor.* **2019**, *201*, 13–30. [CrossRef]

32. Blaser, P.; Zimmermann, S.; Luster, J.; Shotyk, W. Critical examination of trace element enrichments and depletions in soils: As, Cr, Cu, Ni, Pb, and Zn in Swiss forest soils. *Sci. Total Environ.* **2000**, *249*, 257–280. [CrossRef]

33. Desaules, A. Critical evaluation of soil contamination assessment methods for trace metals. *Sci. Total Environ.* **2012**, *426*, 120–131. [CrossRef]

34. Wu, J.; Teng, Y.; Lu, S.; Wang, Y.; Jiao, X. Evaluation of soil contamination indices in a mining area of Jiangxi, China. *PLoS ONE* **2014**, *9*, e112917. [CrossRef]

35. Maanan, M.; Saddik, M.; Maanan, M.; Chaibi, M.; Assobhei, O.; Zourarah, B. Environmental and ecological risk assessment of heavy metals in sediments of Nador lagoon, Morocco. *Ecol. Indic.* **2015**, *48*, 616–626. [CrossRef]

36. Rachwał, M.; Kardel, K.; Magiera, T.; Bens, O. Application of magnetic susceptibility in assessment of heavy metal contamination of Saxonian soil (Germany) caused by industrial dust deposition. *Geoderma* **2017**, *295*, 10–21. [CrossRef]

37. Leach, D.L.; Viets, J.G.; Powell, J.W. Textures of ores from the Silesian-Cracow zinc-lead deposits, Poland: Clues to the ore-forming environment. *Pol. Geol. Inst. Pap.* **1996**, *154*, 37–50.

38. Szuwarzynski, M. Ore bodies in the Silesian-Cracow Zn-Pb ore district, Poland. *Pol. Geol. Inst. Pap.* **1996**, *154*, 9–24.

39. Górecka, E. Mineral sequence development in the Zn-Pb deposits of the Silesian-Cracow area, Poland. *Pol. Geol. Inst. Pap.* **1996**, *154*, 37–50.

40. Molenda, D. *Mining of Lead and Silver in the Silesia-Cracow Region Up to the Middle of the 16th Century*; Ossolineum: Wrocław, Poland, 1963.

41. Panek, S. The History of Lead and Zinc Ore Mining in Jaworzno-Trzebinia-Chrzanow. Unpublished work, Jaworzno. 1995.

42. Cabala, J.; Sutkowska, K. Past exploitation and processing of Zn-Pb ore influence on the industrial soil minerals composition. Olkusz and Jaworzno district. *Pr. Nauk. Inst Górnictwa Polit Wrocł Studia Mater.* **2006**, *117*, 13–22.

43. Sutkowska, K.; Teper, L. Anthropogenic forms of urban post-mining landscape by example of Jaworzno. *Prz. Górn.* **2012**, *68*, 70–77.

44. Teper, E. Dust-particle migration around flotation tailings ponds: Pine needles as passive samplers. *Environ. Monit. Assess.* **2009**, *154*, 383–391. [CrossRef] [PubMed]

45. Aleksander-Kwaterczak, U.; Helios-Rybicka, E. Contaminated sediments as a potential source of Zn, Pb, and Cd for a river system in the historical metalliferous ore mining and smelting industry area of South Poland. *J. Soils Sediments* **2009**, *9*, 13. [CrossRef]

46. Aleksander-Kwaterczak, U.; Ciszewski, D.; Szarek-Gwiazda, E.; Kwandrans, J.; Wilk-Woźniak, E.; Waloszek, A. The influence of historical activity of the Zn-Pb ore mine in Chrzanów on the aquatic environment quality of the Matylda valley. *Górnictwo Geol.* **2010**, *5*, 21–30.

47. Chlopecka, A.; Bacon, J.R.; Wilson, M.J.; Kay, J. Forms of Cadmium, Lead and Zinc in contaminated soils from Southwest Poland. *J. Environ. Qual.* **1996**, *25*, 69–79. [CrossRef]

48. Cabala, J.; Teper, L. Metalliferous constituents of rhizosphere soils contaminated by Zn-Pb mining in southern Poland. *Water Air Soil Pollut.* **2007**, *178*, 351–362. [CrossRef]

49. Sutkowska, K.; Teper, L.; Vaněk, A.; Czech, T.; Baran, A. Effect of historical zinc processing on soil: A case study in Southern Poland. In Proceedings of the 3rd World Congress on New Technologies (NewTech'17), Rome, Italy, 6–8 June 2017; p. 110. [CrossRef]

50. Vaněk, A.; Chrastný, V.; Teper, L.; Cabala, J.; Penížek, V.; Komárek, M. Distribution of thallium and accompanying metals in tree rings of Scots pine (*Pinus sylvestris* L.) from a smelter-affected area. *J. Geochem. Explor.* **2011**, *108*, 73–80. [CrossRef]

51. Pająk, M.; Halecki, W.; Gąsiorek, M. Accumulative response of Scots pine (*Pinus sylvestris* L.) and silver birch (Betula pendula Roth) to heavy metals enhanced by Pb-Zn ore mining and processing plants: Explicitly spatial considerations of ordinary kriging based on a GIS approach. *Chemosphere* **2017**, *168*, 851–859. [CrossRef]

52. Augustyniak, M.; Orzechowska, H.; Kędziorski, A.; Sawczyn, T.; Doleżych, B. DNA damage in grasshoppers' larvae—Comet assay in environmental approach. *Chemosphere* **2014**, *96*, 180–187. [CrossRef]

53. Dmowski, K.; Rossa, M.; Kowalska, J.; Krasnodębska-Ostręga, B. Thallium in spawn, juveniles, and adult common toads (Bufo bufo) living in the vicinity of a zinc-mining complex, Poland. *Environ. Monit. Assess.* **2015**, *187*, 4141. [CrossRef]

54. Kurek, S.; Sobczyński, P.; Szuwarzyński, M.; Wojnar, E. The characteristics of the Chrzanow region deposits. *Pol. Geol. Inst. Pap.* **1977**, *45*, 45–71.

55. Håkanson, L. An ecological risk index for aquatic pollution controls sediment logical approach. *Water Res.* **1980**, *14*, 975–1001. [CrossRef]

56. Tomlinson, D.L.; Wilson, J.G.; Harris, C.R.; Jeffrey, D.W. Problems in the assessment of heavy-metal levels in estuaries and the formation of a pollution index. *Helgol. Wiss. Meeresunters.* **1980**, *33*, 566–575. [CrossRef]

57. Zhang, C.; Qiao, Q.; Piper, D.; Huang, B. Assessment of heavy metal pollution from a Fe-smelting plant in urban river sediments using environmental magnetic and geochemical methods. *Environ. Pollut.* **2011**, *159*, 3057–3070. [CrossRef] [PubMed]

58. Müller, G. Index of geo-accumulation in sediments of the Rhine River. *Geo. J.* **1969**, *2*, 108–118.

59. Detailed Geochemical Map of Upper Silesia. *Sheet: Sławków, Olkusz, Nowa Góra, Myślachowice, Chrzanów, Dabrowa Górnicza, Strzemieszyce, Jaworzno and Libiąż*; Pasieczna, A., Ed.; Polish Geological Institute: Warszawa, Poland, 2008.

60. Lis, J.; Pasieczna, A. *Geochemical Atlas of Upper Silesia 1:200,000*; Publications of the Polish Geological Institute: Warszawa, Poland, 1995.

61. Salminen, R. (Ed.) *Geochemical Atlas of Europe 2005 Part 1 and 2*; Geol. Survey of Finland: Espoo, Finland, 2005.

62. Sutherland, R.A.; Tolosa, C.A.; Tack, F.M.G.; Verloo, M.G. Characterization of Selected Element Concentrations and Enrichment Ratios in Background and Anthropogenically Impacted Roadside Areas. *Arch. Environ. Contam. Toxicol.* **2000**, *38*, 428–438. [CrossRef] [PubMed]

63. Gupta, S.; Jena, V.; Matic, N.; Kapralova, V.; Solanki, J.S. Assessment of geo-accumulation index of heavy metal and source of contamination by multivariate factor analysis. *Int. J. Hazard. Mater.* **2014**, *2*, 18–22.

64. Szuszkiewicz, M.; Łukasik, A.; Magiera, T.; Mendakiewicz, M. Combination of geo- pedo- and technogenic magnetic and geochemical signals in soil profiles Diversification and its interpretation: A new approach. *Environ. Pollut.* **2016**, *214*, 464–477. [CrossRef]

65. Szuszkiewicz, M.; Petrovsky, E.; Łukasik, A.; Gruba, P.; Grison, H.; Szuszkiewicz, M.M. Technogenic contamination or geogenic enrichment in Regosols and Leptosols? Magnetic and geochemical imprints on topsoil horizons. *Geoderma* **2021**, *381*, 114685. [CrossRef]

66. Kabata-Pendias, A.; Pendias, H. *Biogeochemistry of Trace Elements*; PWN: Warszawa, Poland, 1999.
67. Romero-Baena, A.J.; González, I.; Galán, E. Soil pollution by mining activities in Andalusia (South Spain)—The role of mineralogy and geochemistry in three case studies. *J. Soils Sediments* **2018**, *18*, 2231–2247. [CrossRef]

Publisher's Note: MDPI stays neutral with regard to jurisdictional claims in published maps and institutional affiliations.